The influence of Ultraviolet-Ozone irradiation time on structural and optical properties of SnO_2 thin films deposited using the slot-die method

F.V. Molefe[1,2], T.E. Seimela[2], N.N. Nyangiwe[1], M. Msimanga[1], M. Diale[2]

[1]Department of Physics, Tshwane University of Technology, Pretoria, South Africa
[2]Department of Physics, University of Pretoria, Pretoria, South Africa

E-mail: Mmantsae.diale@up.ac.za

Abstract. Tin (IV) oxide (SnO_2) is a promising metal oxide (MO) semiconductor with potential in perovskite solar cells (PSCs) as an electron transport layer (ETL). The development of an additive-free SnO_2 thin film with enriched optical properties using a cost-effective method is still a challenge. Herein, we report the influence of Ultraviolet-ozone (UVO) at different irradiation times, ranging from 2.5 min to 5 min, on SnO_2 thin films. The additive-free hydrothermally synthesized SnO_2 thin films were deposited on an FTO substrate using the slot-die method. The thin films were characterised using a range of analytical techniques to evaluate their structural and optical properties. X-ray diffraction (XRD) confirmed SnO_2 crystallization into the tetragonal cassiterite phase. The surface irradiation of SnO_2 thin films with UVO led to an increase in average crystallite size. Variation in the bandgap energy was observed following distinct changes in optical absorption upon UVO-irradiation. The photoluminescence (PL) studies revealed the enhancement in defect emission intensity following an increase in UVO-irradiation time. These findings emphasize the significance of UVO-irradiation in tuning the optical properties of SnO_2 thin films for application as an ETL in PSCs.

1 Introduction

This document has instructions for writing your For several decades, photovoltaic (PV) devices have been considered viable methods of producing renewable energy and trusted to replace fossil fuels. Several renewable technologies have been explored such as geothermal, solar, and wind [1]. PV devices such as perovskite solar cells (PSCs) and organic solar cells (OSCs) have encountered challenges associated with the transition from laboratory to industrial scale [2]. Thin film devices for these technologies rely solely on the solution-processed materials.

PV devices use the bulk heterojunction (BHJ) configuration to separate excitons at the donor/acceptor interface [3]. This configuration is highly favoured due to the reported impressive power conversion efficiency (PCE) of 25.5 % in PSCs [4]. The efficiency, cost-effectiveness, flexibility, and lightweight construction make PSCs a viable alternative to silicon-based SCs [5]. In traditional n-i-p architecture, PV devices use inorganic metal oxides (MOs) such as CuO, SnO_2, TiO_2, and ZnO etc. as indispensable electron transport layers (ETLs) to achieve high performance [6]. The ETL in PSCs plays a vital role in functioning, stability, scalability and the efficiency as it allows extraction of electrons from the perovskite layer while blocking holes. Organic ETL materials such as carbazole-based PACs have been explored due to their excellent charge transportation through which over 25% efficiency has been achieved [7]. However, they lack long-term stability at high

temperatures and under ultraviolet illumination, which can hinder their application in PV devices hence inorganic MOs are highly favoured.

It should be noted that MOs demonstrate the greatest potential due to their high transparency, conductivity and user-friendly preparation approaches. A significant shift from TiO_2 to SnO_2 as the preferred ETL has been reported [8]. This is due to misalignment of TiO_2 with perovskite materials, leading to enhanced exciton recombination, which has a negative effect on device performance. Among MOs, SnO_2 has extraordinary electron mobility ($240 cm^2V^{-1}s^{-1}$) and compatible band alignment with perovskite materials that alleviate charge transportation at a reduced recombination rate [9]. However, the presence of metal-vacancy defects on the surface causes deterioration of device stability and efficiency. Such defects tend to trap photogenerated carriers and hinder the charge transfer process. Other researchers pretreated SnO_2 precursors with water-soluble polymers to modify its interface in PSCs [10]. Moreover, various process parameters during deposition such as annealing, thickness, and time were explored leaving out post-treatment of the films. Thus, it is desirable to expose thin films to radiation as a way of passivation and reducing surface defects.

The performance ETL within the SC device rely on several factors like the specific surface area (SSA) and operation environment [11]. The preparation and design of ETL with large SSA and extraordinary charge transfer of high significance. SnO_2 can be prepared using various synthesis methods i.e. chemical precipitation, hydrothermal, and solvothermal reaction to produce different structures and shapes (nanoflower, nanoneedle etc.). For over a decade, research has mainly focused on using the spin coater to deposit MOs for SC applications. However, other solution-based deposition methods have been developed such as blade coating, dip coating, slot-die coating and spray coating [12]. Some deposition techniques have numerous issues associated with cost, stability, and reproducibility. Bu et al. demonstrated the feasibility of using the slot-die coating as the most successful method for large area mass production of solution-processed films [13]. Slot-die is a prevalent wet chemical deposition method that is operated at ambient environment to deposit a variety of materials desirable for optoelectronic applications [14]. It has the potential for scaling up the deposition of different essential layers for PSCs.

The primary goal of this study is to undertake the preliminary endeavour in growing SnO_2 thin films using the slot-die coater. The effect of UVO-irradiation time is investigated to gain insights into the structural and optical properties. The SnO_2 thin films were treated with UVO for 2.5 and 5 min after annealing. A significant change in structural and optical properties was observed. UVO-irradiation considerably improved the crystallite size and structural disorder, thereby minimizing the oxygen vacancies and enhancing the optical transmittance. UVO treatment has proven to be technologically efficient in producing SnO_2 with reduced defect density, desirable for PSCs as effective ETL.

2 Experimental

2.1 Materials

The precursors were procured from Sigma-Aldrich Pty. Ltd., South Africa and used in their analytical grade state without further purification. The reagents used for the preparation of SnO_2 nanoparticles were tin tetrachloride (IV) pentahydrate ($SnCl_4 \cdot 5H_2O$ 98%) and ammonium hydroxide (NH_4OH, 28-30%).

2.2 Materials synthesis

The SnO_2 nanoparticles were synthesized as follows: 4g $SnCl_2 \cdot 5H_2O$ was dissolved in 60 ml of ethanol and 20 ml of deionised (DI) water. An NH_4OH solution was added dropwise while continuously stirring using a magnetic hotplate until the pH was adjusted to 14. The obtained solution mixture was transferred into a Teflon autoclave (60 ml) and heated at 200°C for 24 hrs. After cooling, the product was thoroughly washed with ethanol and DI water using a centrifuge to remove residues.

2.3 Thin film deposition

The 12 mm × 12 mm FTO substrates were cleaned sequentially for 10 min in a Sonic-Clean Labotec ultrasonic bath using Sunlight detergent solution, ethanol, and deionised (DI) water. The substrates were blow-dried using nitrogen (N_2) gas, followed by UVO cleaning for 10 min and fixed on a slot die hot plate prior to deposition. The slot-die coating was performed using Ossilla (L2005A1) coater at the speed of 0.5 mm/s, dispense rate 5 uL/s with the substrate preheated to 80°C. The downstream coating gap (hd) was retained at ~0.1 mm. The as-deposited SnO_2 thin films were annealed at 550°C for 2 hrs and exposed to UVO-irradiation for different times (2.5 and 5 min) at room temperature.

2.4 Thin film characterization

The phase identification and purity were probed using Bruker D2 phaser XRD (Cu-K_α radiation, λ=1.5418 Å, 40 kV, 30 mA at a scanning speed of 0.05°/min. The absorption characteristics were measured using an Agilent Cary 60 BIO ultraviolet-visible (UV-Vis) spectrophotometer. A fluorescence spectrophotometer (Hitachi F-7000) equipped with a 150 W xenon arc lamp was used to acquire luminescence measurements.

3 Results and discussion

3.1 Structural analysis

Figure 1(a) shows the XRD diffractograms of as-deposited and UVO-irradiated SnO_2 thin films acquired in the 2θ range 20 - 60°. The as-deposited thin film exhibited a poor crystalline phase of SnO_2 with characteristic peaks at 26.6°, 33.6°, 37.9°, 51.7°, 54.4° and 56.8°. The observed diffraction peaks align well with the tetragonal rutile phase (cassiterite) from reference JCPDS#41-1445 [15], without impurities from precursors. The diffractions marked with asterisks (✯) are associated with the fluorine-doped tin oxide (FTO) substrate used. Moreover, the diffractions marked with the sun (☼) at 37.7°, ~54.6°, and ~56.7° become more apparent with an increase in UVO-irradiation time. The crystallite size of the thin films was estimated using the Debye-Scherrer equation, adopting the (110) and (101) dominant and resolved peaks [16]. The obtained values for the as-deposited, 2.5 and 5 min irradiated thin films were 5.93, 6.68, and 6.84 nm, respectively. These values indicate that UVO-irradiation led to an increase in crystallite size.

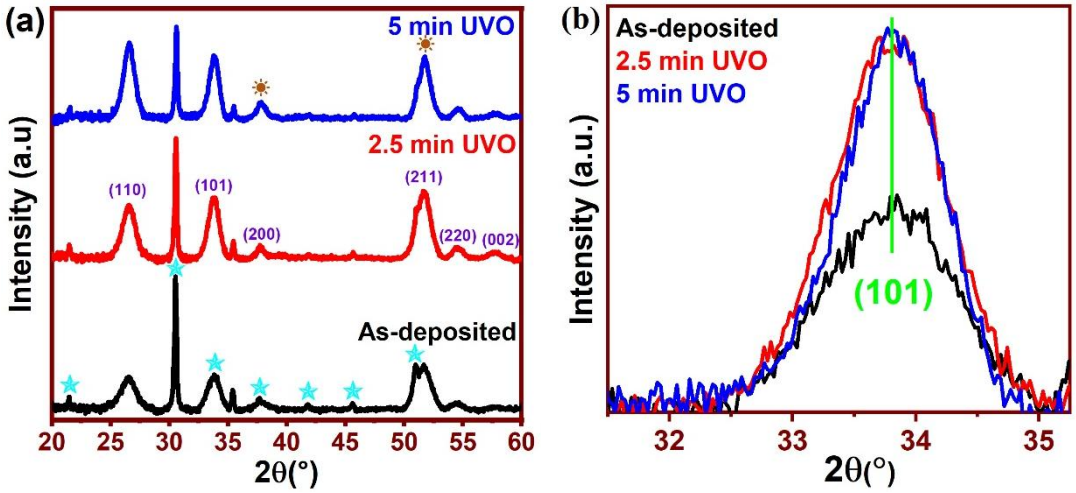

Figure 1: (a) XRD spectra of as-deposited and UVO-irradiated SnO2 thin films, (b) close inspection of the (101) XRD peak.

An enlarged view of the (101) reflection for the as-deposited and UVO-irradiated thin films is presented in Figure 1(b). Upon UVO-irradiation, there is no appreciable peak shifting, indicating that oxygen ions were well incorporated into the SnO_2 crystal lattice and did not cause the structural distortions. Notably, there is an increase in diffraction intensity for the UVO-irradiated thin films, indicative of improved crystallinity.

3.2 Optical analysis

The UV-Vis absorption spectra of as-deposited and UVO-irradiated SnO_2 thin films are presented in Figure 2(a). The as-deposited thin film exhibited significant absorption at ~305 nm in the ultraviolet region, distinctive of an electron transfer from the valence band (VB) to the conduction band (CB) in SnO_2 [17]. A decline in absorbance is observed throughout the entire spectral region, concurrent with the shift to the lower wavelengths. The reduction in absorbance is associated with an increase in transmittance. This is caused by improved crystallinity, which minimizes grain boundaries that scatter light, thereby allowing the photons to be transmitted through the lattice [18]. The observed blueshift represents the modification of the electronic states of SnO_2 by UVO-

irradiation.

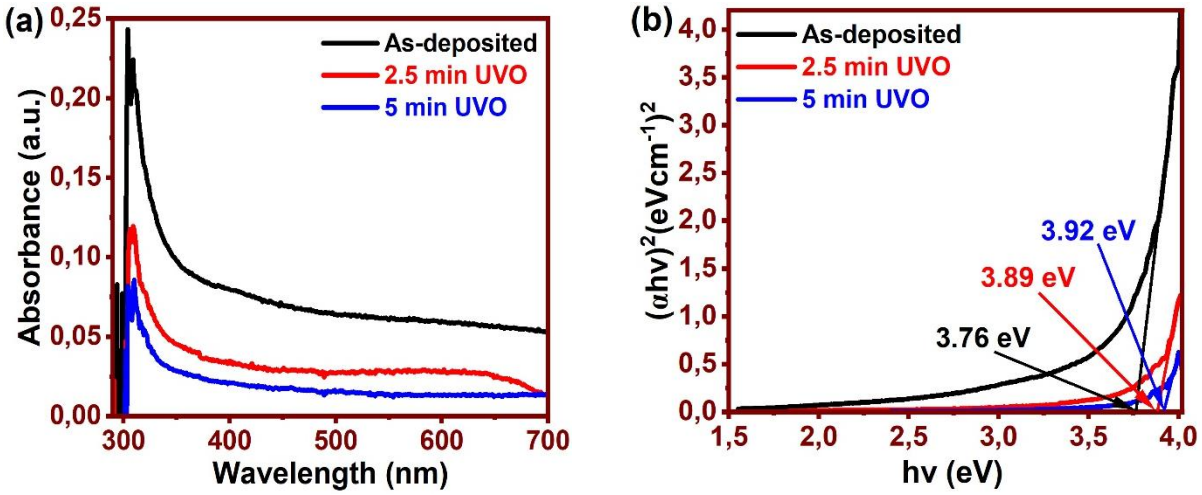

Figure 2: (a) Absorption spectra and (b) plot of $(\alpha hv)^2$ vs (hv) for the as-deposited and UVO-irradiated SnO_2 thin films.

Figure 2(b) shows the optical energy bandgap (E_g) estimated using the Tauc's plot based on the relation $(\alpha hv)^n$ vs hv due to the direct transition n = 2, by extrapolating $(\alpha hv)^2$ to 0 [19]. The values of optical E_g increase with an increase in UVO-irradiation time. An E_g increase indicates the enhancement of transparency in the visible region while maintaining strong electrical conductivity, which is beneficial for ETL in PSCs [20]. This is attributed to the Burstein–Moss effect, due to an increase in free carrier concentration occupying the lower energy states in the CB [21]. The behaviour suggests that UVO-irradiation strengthens the interatomic bonding. Further analysis of absorption characteristics is conducted by determining the Urbach energy (E_U), thereby probing the localized defect levels in the E_g using equation (1):

$$\alpha = \alpha_0 + \exp\left(\frac{hv}{E_U}\right), \quad (1)$$

where α is the absorption coefficient, α_0 represents the pre-exponential factor, and E_U denotes the band tail energies. The E_U values are estimated by applying the natural logarithm to equation (1) and taking the reciprocal of the slope of the linear fit below the E_g from the plot of $ln(\alpha)$ vs hv presented in Figure 3(a). The values of E_U decrease with an increase in UVO-irradiation time. Thus, UVO-irradiation reduces the structural disorder, which represents a better atomic arrangement and less internal stress [22].

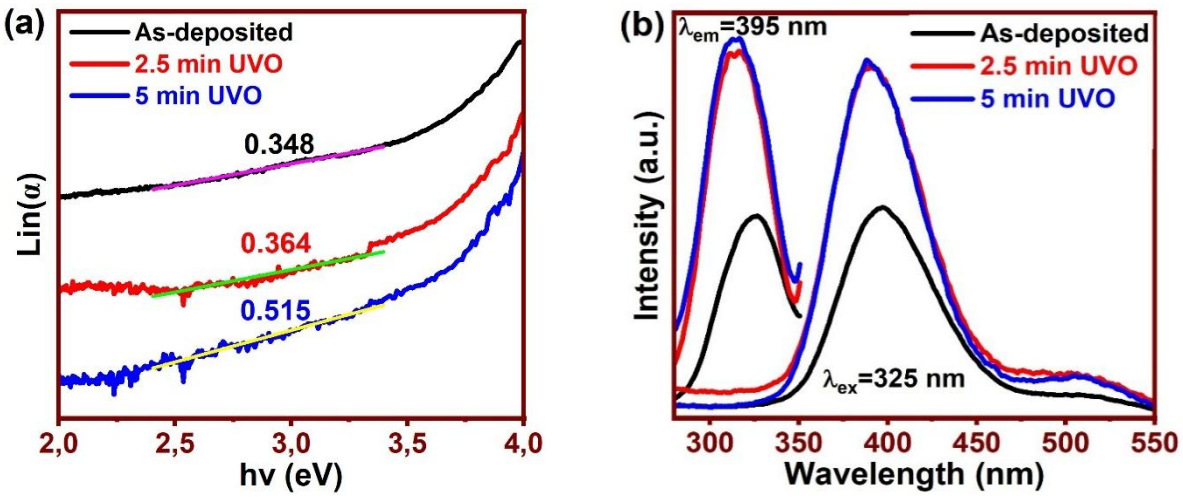

Figure 3: (a) Ln(α) vs hv (b) PL Excitation and Emission spectra of as-deposited and UVO-irradiated SnO_2 thin films.

Figure 3(b) illustrates the excitation and emission characteristics of the as-deposited and UVO-irradiated SnO_2 thin films. The optimal excitation was achieved at λ_{ex}=325 nm and used to monitor the emission obtained at λ_{em}=395 nm. The excitation spectra show a strong absorption, which should be ascribed to the transition of electrons from the VB to the CB in SnO_2. The as-deposited and UVO-irradiated thin films exhibit well-defined emissions peaking in the ultraviolet region (340 – 470 nm) and green region (470 – 550 nm). Generally, PL emission of SnO_2 thin films emanates from various intrinsic defects such as tin interstitials (Sn_i), oxygen vacancies (V_O) and dangling bonds [23]. Upon UVO-irradiation for 2.5 min, the emission intensity at 395 nm progressively increased, and at 5 min of irradiation, there was an insignificant change. This emission is ascribed to an electron transition from the lower edge of the CB to the doubly ionized V_O^{2+} situated above the VB [24]. Similarly, the 509 nm peak resembled an enhancement in the intensity with UVO-irradiation. This emission represents the creation of singly ionized (V_O^+) [25]. According to Ahmed *et al.* [26], the negatively charged oxygen develops a repulsive force and produce an acceptor state (holes) by shifting the VB levels upper into the forbidden gap. Owing to a weak repulsive force, an acceptor energy level is introduced by V_O^+, which causes the recombination of electrons trapped at V_O^+ with holes produced in the VB. This leads to an increase in 509 nm emission mediated by V_O^+. It can be concluded that 5 min UVO-irradiation time is optimal for achieving high intensity, with the likelihood of reduced intensity for longer irradiation times. It is well noted that excitation and emission spectra are slightly blueshifted, and this agrees well with the E_g widening observed in the absorption results. Thus, V_O defects were minimised, symbolising the enhancement of thin film quality through the increase in oxygen density. The increase in emission intensity indicates a delay in the recombination rate, which is vital for an ETL towards more photogenerated electron-hole pair generation and charge transfer.

4 Conclusion

The influence of UVO-irradiation time on SnO_2 thin films grown using the slot-die method was successfully investigated. The thin film properties were studied using XRD, UV-Vis, and PL techniques. The UVO-irradiated thin films revealed an increase in crystallite size with an increase in UVO-irradiation time. There was a substantial variation in E_g upon increasing UVO-irradiation time, which signified the changes in defect states and light transmission. An estimated E_U was reduced with the increase in UVO-irradiation time, suggesting lessened crystal disorder and defect density. The PL emission revealed a reduction in O defects upon increasing the UVO-irradiation time. Thus, the improved structural and optical properties are attributed to enhanced transmittance and reduced recombination losses. These discoveries underscore the importance of UVO-irradiation and provide guidelines for developing effective ETL for PSCs.

Acknowledgements

The authors thankful for the financial support of the project provided by the University of Pretoria (UP) Physics Department through the National Research Foundation (NRF) - South African Research Chairs Initiative (SARChI), UID: 115463. Additionally, the support from Tshwane University of Technology (TUT) for conference attendance is highly appreciated.

References

[1] L. Wang and J. Pang, “Assessing the impact of climate mitigation technology and environmental tax on renewable energy development: A dynamic threshold approach,” *Renew Energy*, vol. 244, p. 122683, May 2025, doi: 10.1016/j.renene.2025.122683.

[2] R. Keshavarzi *et al.*, “Organic and perovskite solar cells based on scalable slot-die coating technique: Progress and challenges,” Apr. 01, 2025, *Elsevier B.V.* doi: 10.1016/j.nantod.2024.102600.

[3] P. Bi *et al.*, “Donor-acceptor bulk-heterojunction sensitizer for efficient solid-state infrared-to-visible photon up-conversion,” *Nature Communications* , vol. 15, no. 1, Dec. 2024, doi: 10.1038/s41467-024-50177-4.

[4] L. Chen *et al.*, “Non-ionic polymeric polyacrylamide (PAM) modified SnO2 electron transport layer for high-efficiency perovskite solar cells,” Aug. 01, 2024, *Elsevier B.V.* doi: 10.1016/j.solmat.2024.112907.

[5] A. Chandrakar and A. Khare, “A comprehensive review of flexible perovskite solar cells: Materials, mechanisms, properties, applications, and commercialization status,” Sep. 15, 2025, *Elsevier Ltd*. doi: 10.1016/j.solener.2025.113649.

[6] Q. Zhang *et al.*, “Multifunctional organic molecule with synergistic modified SnO2 for efficient perovskite solar cells,” *J Alloys Compd*, vol. 1010, Jan. 2025, doi: 10.1016/j.jallcom.2024.177653.

[7] X. Cui *et al.*, “Promising Cobalt Oxide Hole Transport Layer for Efficient and Stable Inverted Perovskite Solar Cells,” *Adv Funct Mater*, Feb. 2025, doi: 10.1002/adfm.202425119.

[8] C. Yan *et al.*, “Influence of surface groups on SnO2 nanoparticles in enhancing perovskite photodetector performance,” *Org Electron*, vol. 138, Mar. 2025, doi: 10.1016/j.orgel.2024.107194.
[9] R. Panyathip *et al.*, “Surface modification of SnO2 electron transporting layer by graphene quantum dots for performance and stability improvement of perovskite solar cells,” *Ceram Int*, vol. 50, no. 19, pp. 34840–34848, Oct. 2024, doi: 10.1016/j.ceramint.2024.06.293.
[10] Y. Wang *et al.*, “Poly(acrylic acid)-modified SnO2/CdS double electron transport layers for efficient and stable Sb2(S,Se)3 solar cells,” *Solar Energy Materials and Solar Cells*, vol. 281, Mar. 2025, doi: 10.1016/j.solmat.2024.113322.
[11] C. Luo *et al.*, “SnO2 mesoporous nanostructures serve as battery-type cathode for hybrid supercapacitor with superior electrochemical performance,” *Colloids Surf A Physicochem Eng Asp*, vol. 712, May 2025, doi: 10.1016/j.colsurfa.2025.136440.
[12] R. Patidar, D. Burkitt, K. Hooper, D. Richards, and T. Watson, “Slot-Die Coating of Perovskite Solar Cells: An Overview.”
[13] T. Bu *et al.*, “Universal passivation strategy to slot-die printed SnO 2 for hysteresis-free efficient flexible perovskite solar module,” *Nat Commun*, vol. 9, no. 1, Dec. 2018, doi: 10.1038/s41467-018-07099-9.
[14] Y. Bouachiba *et al.*, “An investigation into the effect of Gd on the optoelectronic properties of ZnO waveguide thin films by prism coupler,” *J Lumin*, vol. 275, Nov. 2024, doi: 10.1016/j.jlumin.2024.120740.
[15] P. Kamakshi, C. Joshitha, S. Chella, and G. Kumar K, “Enhancing photocatalytic applications with SnO2/Ti3C2 Mxene nanocomposite: Synthesis and characterization,” *Chem Phys Lett*, vol. 833, Dec. 2023, doi: 10.1016/j.cplett.2023.140945.
[16] F. V Molefe, L. F. Koao, B. F. Dejene, and H. C. Swart, *Influence of zinc acetate concentration in the preparation of ZnO nanoparticles via chemical bath deposition*.
[17] H. A. Alali, F. Tiss, K. Omri, K. Alamer, and Z. H. Alhashem, “Effect of Mn doping on microstructure and photocatalytic properties of ZnO nanoparticles synthesized via a hydrothermal method,” *Mater Res Express*, vol. 11, no. 12, Dec. 2024, doi: 10.1088/2053-1591/ad9fd8.
[18] M. A. Sayeed and H. K. Rouf, “Al-doped SnO2 thin films: impacts of high temperature annealing on the structural, optical and electrical properties,” *Journal of Materials Research and Technology*, vol. 15, pp. 3409–3425, Nov. 2021, doi: 10.1016/j.jmrt.2021.09.145.
[19] A. Alsulami and A. Alsalme, “Enhancement of the structural, optical, and optoelectrical properties of nebulizer spray pyrolyzed SnO2 thin films by strontium doping,” *Physica B Condens Matter*, vol. 699, Feb. 2025, doi: 10.1016/j.physb.2024.416783.
[20] D. Bouras *et al.*, “Enhanced CO2 sensing properties of Fe/Al-doped SnO2 thin films: A comprehensive study of structural, optical, and electrical characteristics,” *J Alloys Compd*, vol. 1034, Jun. 2025, doi: 10.1016/j.jallcom.2025.181387.
[21] M. A. Bezzerrouk *et al.*, “Effect of Sr doping on microstructure, morphology, photoluminescence, optical properties and photocatalytic performance of SnO2 thin films,” *Opt Mater (Amst)*, vol. 167, Oct. 2025, doi: 10.1016/j.optmat.2025.117292.
[22] C. Muiva, D. P. Sebuso, and E. Muchuweni, “Microstructural and optical properties of nanostructured Al/Ag co-doped ZnO thin films (AgxAl0.03ZnO0.97-x) by spray pyrolysis for optoelectronic applications,” *Physica B Condens Matter*, vol. 690, Oct. 2024, doi: 10.1016/j.physb.2024.416206.
[23] P. Asha Hind, P. Kumar, U. K. Goutam, and B. V. Rajendra, “Tuning of electrical properties and persistent photoconductivity of SnO2 thin films via La doping for optical memory applications,” *Mater Sci Semicond Process*, vol. 186, Feb. 2025, doi: 10.1016/j.mssp.2024.109073.
[24] B. Teldja, B. Noureddine, B. Azzeddine, and T. Meriem, “Effect of indium doping on the UV photoluminescence emission, structural, electrical and optical properties of spin-coating deposited SnO2 thin films,” *Optik (Stuttg)*, vol. 209, May 2020, doi: 10.1016/j.ijleo.2020.164586.
[25] A. Ahmed, T. Ali, M. Naseem Siddique, A. Ahmad, and P. Tripathi, “Enhanced room temperature ferromagnetism in Ni doped SnO2 nanoparticles: A comprehensive study,” *J Appl Phys*, vol. 122, no. 8, Aug. 2017, doi: 10.1063/1.4999830.
[26] A. Ahmed, M. Naseem Siddique, U. Alam, T. Ali, and P. Tripathi, “Improved photocatalytic activity of Sr doped SnO 2 nanoparticles: A role of oxygen vacancy,” *Appl Surf Sci*, vol. 463, pp. 976–985, Jan. 2019, doi: 10.1016/j.apsusc.2018.08.182.